geoconvention
Calgary • Canada • May 13-17 2019

Coherence cube analysis via a 3D Riesz transform

Bernal Manzanilla Saavedra and Mauricio D. Sacchi

Department of Physics, University of Alberta

Summary

In the classical theory of analytic signals, a trace is decomposed into an amplitude envelope and a phase via the Hilbert transform. However, this is a trace-by-trace process that does reflect multi-trace patterns that exist in 3D seismic data cubes. In this work we present the use of the 3D Riesz transform to calculate a 3D analytic signal for attribute analysis of seismic cubes.

Introduction

In Taner et al. (1979) a complex trace is obtained from a real valued trace ($f(t)$) summing the initial signal plus its purely imaginary, $\pi/2$ phase rotated quadrature ($f_H(t)$). The quadrature is obtained from the initial data applying a Hilbert transform. In frequency domain, the Hilbert transform is given by the sign function of the frequency (ω) multiplied by the input trace spectrum. This operator is nothing but a fractional differential operator (Chopra and Marfurt, 2007), meaning

$$f_H(t) = \mathscr{F}^{-1}\{F_H(\omega)\} = \mathscr{F}^{-1}\{-i\frac{\omega}{|\omega|}F(\omega)\} = \mathscr{F}^{-1}\{\frac{1}{|\omega|}\} * \frac{d(f(t))}{dt}\,. \tag{1}$$

However, this decomposition is not adequate for a 2D or 3D signal, since there are two or three directions, respectively, along which the frequency or wavenumber changes sign. In this work we present an extension of our previous work on the 2D Riesz transforms (Manzanilla-Saavedra and Sacchi, 2018) to 3D seismic data sets.

Theory

Let a seismic 3D gather or seismic cube, and its Fourier transform, represented by $f(x_1,x_2,x_3)$ and $F(k_1,k_2,k_3)$. The variable x_2 can represent depth or time and, consequency, k_3 can represent vertical wavenumber of temporal frequency. Similarly, we define the position and wavenumber vectors $\mathbf{x} = (x_1,x_2,x_3)$ and $\mathbf{k} = (k_1,k_2,k_3)$, respectively. The quadrature cube in the *j-th* direction is obtained by multiplying the initial data cube in frequency domain, element by element, times the Riesz kernel $-i\frac{k_j}{|\mathbf{k}|}$ with $j = 1,2,3$ and $|\mathbf{k}| = \sqrt{{k_1}^2+{k_2}^2+{k_3}^2}$. Hence, the Riesz transform is similar to the Hilbert transform in the sense that it is also a fractional differential operator (Chenouard and Unser, 2012) and it is given by

$$f_j{}^R(\mathbf{x}) = \mathscr{F}^{-1}\{-i\frac{k_j}{|\mathbf{k}|}F(\mathbf{k})\} = \mathscr{F}^{-1}\{\frac{1}{|\mathbf{k}|}\} * \frac{\partial}{\partial x_j}f(\mathbf{x})\,,\; j = 1,2,3\,, \tag{2}$$

where the symbol $*$ represent convolution. Each quadrature cube j is of the same size than the initial data, and beyond its differential nature, it has the advantage of not emphasizing high frequencies given the low pass $\frac{1}{|\mathbf{k}|}$ term. We now define a vector field (for the sake of brevity *Riesz vector*), that is collinear with the gradient vector field, and normal to the reflector surfaces in the data

$$\mathbf{g}(\mathbf{x}) = \mathscr{F}^{-1}\{\frac{1}{|\mathbf{k}|}\} * \nabla f(\mathbf{x}) = (f_1{}^R(\mathbf{x}), f_2{}^R(\mathbf{x}), f_3{}^R(\mathbf{x})) \tag{3}$$

Let the first order structure tensor $\mathbf{S}(\mathbf{x})$ be a 3×3 symmetric matrix that can be evaluated at each position in the cube $\mathbf{x}$

$$\mathbf{S}(\mathbf{x}) = E[\mathbf{g}(\mathbf{x})^T\mathbf{g}(\mathbf{x})] \tag{4}$$

The expected value ($E[.]$) of the outer product $\mathbf{g}(\mathbf{x})^T\mathbf{g}(\mathbf{x})$ is replaced by a weighted average in the vicinity of the central point $\mathbf{x}$. A spherical Gaussian smoothing kernel was used as weighting function (Wu, 2017). We extract the 3 eigenvalues of the tensor $\mathbf{S}(\mathbf{x})$ to define coherence (Chenouard and Unser, 2012) , σ_1, σ_2 and σ_3

$$C(\mathbf{x}) = \frac{\sigma_1(\mathbf{x}) - (1/2)[\sigma_2(\mathbf{x}) + \sigma_3(\mathbf{x})]}{\sigma_1(\mathbf{x}) + (1/2)[\sigma_2(\mathbf{x}) + \sigma_3(\mathbf{x})]} \tag{5}$$

The coherence coefficient, $C(\mathbf{x})$, is a measure of how flat the reflectors are, and hence a measure of continuity along a chosen time slice. If the reflector is flat in the vicinity of a given sample the structure tensor becomes rank one and only one singular vector and one singular value explain the Riesz vector in the surroundings of that sample, meaning $\sigma_1(\mathbf{x}) \gg \sigma_2(\mathbf{x}), \sigma_3(\mathbf{x})$ and the coherence is nearly one. On the contrary when reflectors depart from a flat surface or there is no structure in the amplitude distribution, all singular vectors are needed to explain the Riesz vector orientation and the coherence drops to zero.

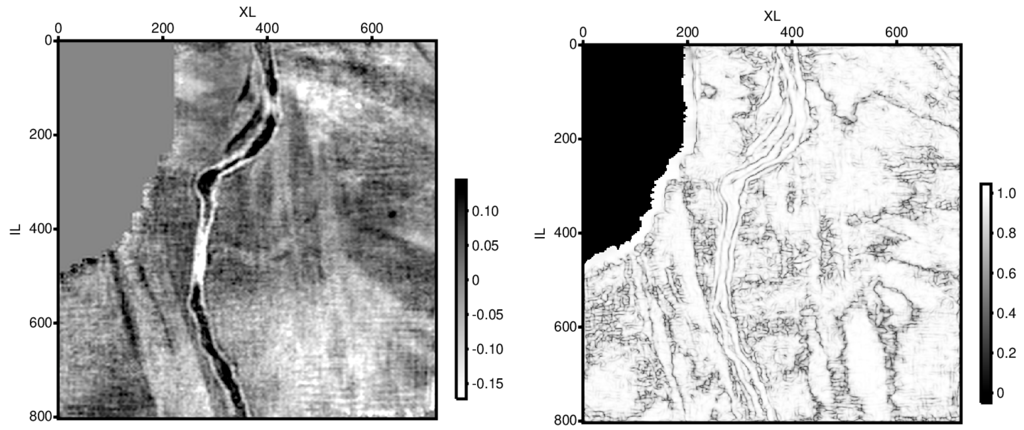

(a) (b)

Figure 1: Coherence for the 0.9(s) time slice. Low coherence is observed around the channel since it is not contained in the reflector plane, specially around its levees.

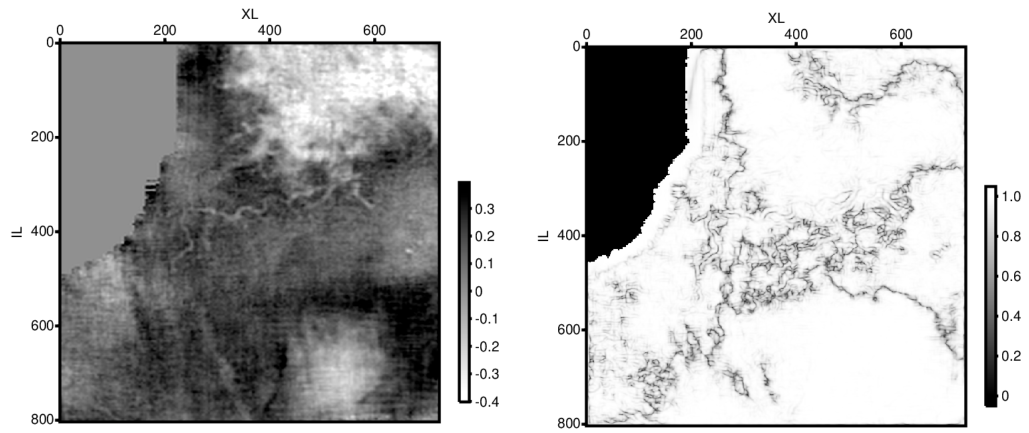

(a) (b)

Figure 2: Coherence for the 2.1(s) time slice. Low coherence is observed around the channel since it is not contained in the reflector plane, specially around its levees.

Results

As examples, we present two target time slices of a migrated data cube of the Western Canadian Basin. The 3D Riesz transform operator is used to estimate the local coherence coefficients for the two target slices. Figure 1a is the time slide extracted at 0.9s from the 3D cube with its associated coherence displayed in Figure 1b. In the coherence time slice, the channel levees and the boundaries of reflectors show very low coherence features as these structures, depart from a flat surface. We repeat the analysis for a time slide at 2.1s and portray the time slice and its coherence in Figures 2a and b, respectively.

Conclusion

We presented an application of the 3D Riesz transform as a fractional differential operator and used it to generate a coherence cube. The Riesz transform allows to define an operator with similar properties to conventional differential operators with the added advantage of having a higher tolerance to noise given the fact that it does not enhance the high frequency content

Acknowledgements

The authors are grateful to the sponsors of Signal Analysis and Imaging Group (SAIG) at the University of Alberta for their continued support.

References

Chenouard, N., and M. Unser, 2012, 3d steerable wavelets in practice: IEEE Transactions on Image Processing, **21**, 4522–4533.

Chopra, S., and K. J. Marfurt, 2007, Volumetric curvature attributes add value to 3d seismic data interpretation: The Leading Edge, **26**, 856–867.

Manzanilla-Saavedra, B., and M. Sacchi, 2018, Monogenic signal in seismic pattern recognition: SEG Technical Program Expanded Abstracts 2018, 1579–1584.

Taner, M. T., F. Koehler, and R. E. Sheriff, 1979, Complex seismic trace analysis: GEOPHYSICS, **44**, 1041–1063.

Wu, X., 2017, Directional structure-tensor-based coherence to detect seismic faults and channels: Geophysics, **82**, A13–A17.